

ANL/RE/CP. - 85929  
CONF-950740--63

The submitted manuscript has been authored by a contractor of the U. S. Government under contract No. W-31-109-ENG-38. Accordingly, the U. S. Government retains a nonexclusive, royalty-free license to publish or reproduce the published form of this contribution, or allow others to do so, for U. S. Government purposes.

## SLOSHING ANALYSIS OF VISCOUS LIQUID STORAGE TANKS

R. Aziz Uras  
Reactor Engineering Division  
Argonne National Laboratory  
Argonne, Illinois

### ABSTRACT

The effect of viscosity on the sloshing response of tanks containing viscous liquids is studied using the in-house finite element computer code, FLUSTR-ANL. Two different tank sizes each filled at two levels, are modeled, and their dynamic responses under harmonic and seismic ground motions are simulated. The results are presented in terms of the wave height, and pressures at selected nodes and elements in the finite element mesh. The viscosity manifests itself as a damping effect, reducing the amplitudes. Under harmonic excitation, the dynamic response reaches the steady-state faster as the viscosity value becomes larger. The fundamental sloshing frequency for each study case stays virtually unaffected by an increase in viscosity. For the small tank case, a 5% difference is observed in the fundamental frequency of the smallest (1 cP) and the highest (1000 cP) viscosity cases considered in this study. The fundamental frequencies of the large tank are even less sensitive.

### INTRODUCTION

There are several environmental concerns related to the high level waste (HLW) storage tanks. One important aspect is the prediction of the sloshing behavior of the waste material and the dynamic response of the storage tanks under seismic excitation. Tests performed in high level waste storage tanks showed that the stored waste material is highly viscous. Thus, it is imperative to determine the effect of viscosity on the dynamic response of tanks filled with viscous fluid under seismic ground motion.

In order to analyze the viscosity effects, studies have been performed using the three-dimensional (3D) finite element computer code (FLUSTR-ANL) developed at the Argonne National Laboratory (ANL). Several cases with different tank

geometries, viscosity values, and various input motions were considered (Tang, et al., 1993).

The present analysis deals with numerical simulation of viscous liquid sloshing of cylindrical tank experiments which were performed at National Research Institute for Earth Science and Disaster Prevention (NIED), Science and Technology Agency (STA) of Japan, and cooperated with the Ishikawajima-Harima Heavy Industries Co., Ltd. (IHI) (Chiba, et al., 1995). One small and one large tank each filled with liquid at two different levels are studied. Each liquid-filled system is excited with a seismic ground motion, and a harmonic input with a frequency equal to its corresponding fundamental sloshing frequency. A total of three different viscosity values are chosen in the seismic response analysis. Low viscosity value is omitted for the harmonic input cases due to the relatively long computational time required to reach the steady state.

The simulations are performed by using the in-house finite element computer code FLUSTR-ANL. The results are presented in terms of wave height at selected points, and pressure at several levels relevant to the experimental setup.

### TEST CONFIGURATION AND SPECIFICATIONS

One small acrylic tank and one large steel tank were used in the experiments (Chiba, et al., 1995). The test specimens were placed on a shaker table, and were filled with liquid at different levels. Level gauges were placed on the liquid surface to measure the wave height, and pressure sensors were used to determine the pressure at several locations. The specifications for the two tank sizes are described in Table 1.

DISTRIBUTION OF THIS DOCUMENT IS UNLIMITED

MASTER

74

## **DISCLAIMER**

**Portions of this document may be illegible in electronic image products. Images are produced from the best available original document.**

## COMPUTER SIMULATIONS

In this section, the finite element code employed in this study is described briefly. The guidelines of the mathematical modeling are given together with a list of the study cases. The input ground motion data is presented, and the simulation results are discussed on a case-by-case basis.

### Brief Description of the FLUSTR-ANL Computer Code

The FLUSTR-ANL (FLUId-STRUcture Interaction) is a three-dimensional (3D) multi-purpose finite element computer code developed at the Argonne National Laboratory. The code is particularly suitable for performing seismic analysis of liquid-filled structures. It has mixed finite fluid elements and an implicit-explicit mesh partition algorithm, and is very efficient for long time-duration seismic analyses. The code has been verified by comparing code predictions with known analytical solutions, such as Housner's solution on sloshing of simple rigid tanks, and Fritz's solution on two concentric cylinders. Validation against experimental data has also been performed (Chang, et al., 1987). The code has been used extensively in the design of LSPB and other large pool type reactors. It has also been employed in the prediction of seismic sloshing and seismic response of LMRs (Chang, et al., 1988).

The code has the capability to implement the Arbitrary Lagrangian Eulerian (ALE) finite element formulations to solve fluid-structure interactions. The merit of ALE is that an arbitrary reference frame can be designed to describe complicated fluid problems where the use of a pure Eulerian or Lagrangian formulation would be very cumbersome, or in certain cases lead to early computational break-down due to extreme mesh entanglement.

Although it is a three-dimensional code, options to handle two-dimensional plane strain, plane stress, and axisymmetric cases are also incorporated. The finite element library consists of continuum, beam, plate or shell type of finite elements to model solids, and structures, and velocity potential or pressure-velocity formulations to handle fluids. Fluid-structure interaction problems can be solved through a desired combination of the structural and fluid elements existing in the code's element library.

The code is capable of generating various forms of mesh internally, and accepts ground acceleration records as input. The system variables, such as displacements, stresses, pressures etc., are stored for the graphical representation of their time-histories, and for mesh plotting. The options for static analysis is available. Two eigenvalue solvers implemented in the code are based on subspace iteration, and Lanczos algorithms.

### Mathematical Models

Finite element models of the small and large tanks are prepared for the in-house computer code FLUSTR-ANL. The models consist of 660 fluid elements based on the pressure-velocity formulation (Tang, et al., 1993). A thin layer of fluid elements are employed to account for the boundary sliding contact condition along the interface between the fluid and the structure. Figure 1 depicts the node and element used for comparisons on the finite element mesh.

The liquid properties used in the simulations of the small and the large tank are those of water and silicone oil. Three different values of viscosity (1 cP, 200 cP, and 1000 cP) are used for the small tank case to demonstrate the influence of the viscosity on the sloshing response under horizontal ground excitation. The specific density and viscosity values were initially provided by NIED, and tabulated in Table 2. It should be noted that silicone oil and drillmate, a polymer solution (non-Newtonian fluid) were used in the experiments (Chiba, et al., 1995). The fluid properties employed in the simulations correspond to that of water (1 cP) and those of silicone oil (200 cP and 1000 cP).

### Input Acceleration Time Histories

Two types of input ground motion are used in this study: El-Centro earthquake record, and harmonic input with frequencies equalling the fundamental and the second sloshing frequency of the fluid-structure system in consideration. The seismic record used in the analysis is a 53.76 second long N-S El-Centro earthquake input with an amplitude of 200 Gal. The fundamental sloshing frequency for each test configuration obtained from the seismic input simulations is used to study the response to harmonic excitation. The amplitude is chosen as  $1 \text{ in/s}^2$  ( $25.4 \text{ mm/s}^2$ ) which assured that the wave height values stay within the linear range in all cases. The simulations are performed until a steady-state response is observed.

### Discussion of Numerical Results

The dynamic response of the small and large tanks each filled at two different liquid levels are simulated for three viscosity values. The computer simulation results are presented for the small tank and the large tank, separately. The effect of viscosity on the response is also discussed for each case. In each case, the time history plots and the corresponding Fast-Fourier Transformation (FFT) for the vertical fluid displacements at a selected node, and the pressure in a selected element are presented to illustrate the results of numerical simulations.

Small Tank. For the small tank, computer simulations are performed for three viscosity values (1 cP, 200 cP, and 1000 cP), and for two liquid depths (39% and 78% of the tank height). The fundamental sloshing frequency for each case is determined from the system's response to the seismic excitation input (Table 3).

In all six cases analyzed, an amplitude of 200 Gal seismic excitation produced maximum wave heights exceeding 10% of the diameter or the liquid depth, a commonly accepted limit for linear response. It is believed that an approach which accounts for the nonlinear behavior of the liquid sloshing is needed to correctly predict the response under relatively high amplitude excitation. The time history plots and the corresponding FFT spectra for the vertical displacements of node 131 and for the pressure in element 1 are given in Figs. 2 and 3 for the 78% full small tanks with liquid viscosities of 1 cP, 200 cP, and 1000 cP, respectively.

For each case, sinusoidal input excitation records are computed with the first and second sloshing frequencies presented in Table

3. Simulations are performed using the same finite element models until a steady-state is reached. Due to the exceptionally long computer run time required for low viscosity liquids to reach the steady state, the 1 cP case is omitted.

A summary of the simulation results for the small tank cases is as follows:

For a given value of viscosity, the fundamental sloshing frequency of the 39% full tank is only slightly different than that of the 78% full tank. A comparison shows that the surface displacements and pressures are higher for the small tank filled with more fluid.

A slight beating phenomenon is observed for the cases studied here. The Fast Fourier Transform (FFT) method is limited by the choice of the time step used in the time-discretization process. The time step used here is computationally feasible, yet is not fine enough to capture the exact fundamental frequency for each of the small tank test cases. Therefore, several cases with small variations in the input frequency have to be considered to determine the actual fundamental frequency.

The sensitivity of the displacements and pressures to a small variation in the input frequency near the second sloshing frequency is relatively low.

The surface displacement is the largest near the tank wall, and decreases toward the center of the tank. This indicates that the viscosity does not affect the sloshing wave form.

The theory and experiments suggest that the pressure values become smaller toward the bottom of the tank in the absence of viscosity. The simulation results, in agreement with the experimental observations, reveal a similar phenomenon for the three values of viscosity studied here.

As mentioned earlier, the fundamental sloshing frequency of each case is relatively unaffected by an increase in viscosity. A 5% difference is observed between the 1 cP, and 1000 cP cases. The difference between the 200 cP and 1000 cP cases is even smaller indicating that the frequency response is rather insensitive.

Due to the damping effect of the viscosity, the wave height and pressure values are smaller for higher viscosity cases provided that all other system characteristics are kept the same. In contrast to the frequency response, the time-dependent response is drastically reduced in higher viscosity cases. The vertical displacements and pressures are reduced by as much as 50% from the 200 cP case to the 1000 cP case (see Table 5). Due to a wide frequency spectrum involved in the seismic excitation case, the reduction appears to be less (see Table 4). The largest influence is observed for the 39% full case where up to 25% reduction in displacements and pressures is encountered.

Large Tank. In the case of the large tank, computer simulations are performed for three viscosity values (1 cP, 200 cP, and 1000 cP), and for two liquid depths (27% and 71% of the tank height). The first and second sloshing frequencies for each case are also determined from the seismic excitation simulation results (Table 4).

In all six cases analyzed, an amplitude of 200 Gal seismic excitation produced maximum wave heights exceeding 10% of the liquid depth, a commonly accepted limit for linear response.

The first and second sloshing frequencies obtained from the seismic analysis are employed to create harmonic input records. Simulations are performed using the same finite element models until a steady-state is reached. Due to the long computer run time required for low viscosity liquids to reach the steady state, the 1 cP case is omitted. Even at 200 cP, the steady state time is of order 110 and 180 seconds for 27% and 71% full tanks, respectively.

A summary of the simulation results for the large tank cases is as follows:

The fundamental sloshing frequency of the 27% full tank is only slightly different than that of the 71% full tank for a given viscosity value. A comparison shows that the surface displacements and pressures are higher for the large tank containing more fluid.

No beating phenomenon is observed for the cases studied here involving the fundamental frequency. The Fast Fourier Transform (FFT) method is limited by the choice of the time step used in the time-discretization process. The time step used here is not only computationally feasible, but is also fine enough to capture the exact fundamental frequency for each of the large tank simulation cases.

The simulation results show that the wave height and pressure are very sensitive to small variations in the input frequency near the second sloshing frequency. Heavy beating and large errors in the time histories are induced.

The surface displacement is the largest near the tank wall, and decreases toward the center of the tank. This indicates that the viscosity does not affect the sloshing wave form.

The theory and experiments suggest that the pressure values become smaller toward the bottom of the tank in the absence of viscosity. The simulation results, in agreement with the experimental observations, reveal a similar phenomenon for the three values of viscosity studied here.

As mentioned earlier, the fundamental sloshing frequency of each case is relatively unaffected by an increase in viscosity. A 4% difference is observed between the 1 cP, and 1000 cP cases for the 27% full tank. The difference between the 200 cP and 1000 cP cases is even smaller indicating that the frequency response is rather insensitive. The fundamental frequency remains the same for all viscosity values in the 71% full tank cases.

When all other system characteristics stay unchanged, the wave height and pressure values are smaller for higher viscosity cases. This can be attributed to the damping effect of the viscosity. In contrast to the frequency response, the time-dependent response is drastically reduced in higher viscosity cases. The vertical displacements and pressures are reduced by as much as 4 times from the 200 cP case to the 1000 cP case. Due to a wide frequency spectrum involved in the seismic excitation case, the reduction appears to be less. The largest influence is observed for the 27% full case where up to 12% reduction in displacements and pressures is encountered.

Equivalent Viscous Damping. The effect of viscosity can be characterized by an equivalent viscous damping ratio. The

viscous damping represents the dissipation of the mechanical energy into thermal energy.

Consider the equation governing the vibrations of a single-degree-of-freedom system

$$\ddot{x} + 2\zeta\omega_n\dot{x} + \omega_n^2x = \omega_n^2u(t)$$

where  $x$  is the displacement,  $\zeta$  is the damping ratio,  $\omega_n$  is the natural frequency, and  $u(t)$  is the external excitation. A superposed dot denotes the time derivative. If the excitation is harmonic, the excitation is given as

$$u(t) = u_o \cos \omega t$$

where  $u_o$  and  $\omega$  are the amplitude and the excitation frequency, respectively. The steady state response for the displacement becomes

$$x = x_o \cos(\omega t + \phi)$$

where  $\phi$  is the phase angle, and  $x_o$  is the response amplitude. The maximum value of  $x_o$  can be evaluated as

$$2\zeta(1-\zeta)^{1/2} = \frac{u_o}{x_o} \quad (1)$$

In Eq. (1),  $x_o$  is obtained from the simulation results, and for the sloshing motion

$$u_o = \frac{2R}{\lambda^2 - 1} \left( \frac{\ddot{x}_o}{g} \right) \quad \lambda = 1.841$$

where  $R$  is the tank radius,  $\ddot{x}_o$  is the harmonic input acceleration amplitude,  $g$  is the gravitational acceleration, and  $\lambda$  is the first root of  $J'_1(\lambda R) = 0$  ( $J_1$  is the Bessel function of order one).

The equivalent viscous damping for the simulations and the experiments are given in Table 5.

**Summary of the Viscosity Effects.** The steady-state value for each case is compared with the other cases to determine the relative effect of viscosity on the system parameters. For both tank sizes, a definite decrease in wave height and pressure values is observed. The sloshing wave form, and the dynamic pressure distribution along the tank wall are not altered by the viscous response. However, the magnitude reduction is observed to be up to 2 times in the small tank case, and 4 times in the large tank case under harmonic excitation if the viscosity is increased from 200 cP to 1000 cP. Under seismic input, the effect is less pronounced amounting to approximately 12-25% change, possibly due to the wide frequency spectrum. The fundamental sloshing frequencies show a very slight sensitivity to variations in viscosity for the small tank, a mere 5% difference between 1 cP and 1000 cP cases. The large tank cases reveal even smaller influence of viscosity. Only 4% difference is observed for the

27% full large tank, whereas the frequencies remained unchanged for the 71% full large tank. The slight beating phenomenon observed in the small tank cases is believed to be the main reason for a larger difference in the fundamental sloshing frequency for different viscosity values.

#### Discussion on Experimental Results and Comparison with Numerical Simulations

A series of experiments were performed to study the sloshing of liquid with different densities under various types of external excitation. A list of test cases are given below:

1. Small tank 78% full with water
2. Small tank 39% full with water
3. Small tank 78% full with water-drillmate solution (viscosity 10 cP)
4. Small tank 78% full with water-drillmate solution (viscosity 200 cP)
5. Small tank 39% full with water-drillmate solution (viscosity 200 cP)
6. Small tank 78% full with water-drillmate solution (viscosity 1000 cP)
7. Small tank 78% full with silicone oil (viscosity 200 cP)
8. Small tank 39% full with silicone oil (viscosity 200 cP)
9. Small tank 78% full with water (39%) and silicone oil (39%, viscosity 200 cP)
10. Large tank 80% full with water (soft roof)
11. Large tank 90% full with water
12. Large tank 80% full with water (short test)
13. Large tank 72% full with water
14. Large tank 30% full with water
15. Large tank 72% full with water-drillmate solution (viscosity 200 cP)
16. Large tank 30% full with water-drillmate solution (viscosity 200 cP)
17. Large tank 72% full with water-drillmate solution (viscosity 1000 cP)

Each test case consisted of four stages:

- a. Sweep test to determine the natural frequencies
- b. Free vibration damping test for the 1st, 2nd, and 3rd sloshing modes
- c. Steady state sinusoidal response test for the 1st and 2nd sloshing modes
- d. Earthquake response test with 200 Gal and 341 Gal input amplitudes for the El-Centro record.

The results of the experiments together with those of the numerical simulations are presented in Table 5. No direct comparison can be made on maximum wave height between the simulations and the experiments with the small tank filled with silicone oil because the wave height gauges drifted and did not provide useful information. A detailed discussion is given below.

The natural frequencies obtained during the sweep tests, the steady state response to a harmonic input with frequencies near

the first and second sloshing frequencies, and the earthquake response with 200 Gal amplitude are used in comparing the experimental findings to the simulation results.

The steady state experiments were performed by applying 30 cycles of excitation with the relevant frequency at several amplitudes. Any response beyond this limit represents the free vibration. Each case within the scope of this study are discussed case by case. The time history plots provided by IHI are inspected to determine the dynamic characteristics. When a clear beat phenomenon is encountered, the envelope period, and the number of cycles within the beating period are read off from the plots. The maximum and minimum response values are also recorded. This procedure is followed for the first and second sloshing frequencies. As indicated above, the experiments were carried out by exciting the fluid-structure system for a duration of 30 cycles at a fixed input frequency. This limited amount of time turns out to be not enough to reach the steady state in some of the cases considered here. For the small tank, 30 cycles would last approximately 30 seconds, if the input frequency is near the first sloshing frequency, and approximately 17 seconds in the case of the second sloshing frequency (refer to Table 6 for a detailed breakdown).

As seen in Table 6, the simulation results for the small tank show that 30 cycles are barely enough to reach the steady state for the 39% full (200 cP).

For the large tank, 30 cycles of the first and second sloshing frequencies take approximately 50-60 seconds, and 30 seconds, respectively. Table 7 presents a summary. It should be noted that the experiments were performed using a large tank filled with 30% and 72% liquid, whereas a 27% and a 71% full large tank were considered in the simulations.

The experimental values for 200 Gal and 341 Gal earthquake input are retrieved to determine if the response shows a nonlinearity. Since the same earthquake record used in the experiments are applied to the computer model, a more reliable comparison can be accomplished.

In the harmonic excitation case, the computer simulations were performed using an acceleration input amplitude of 1 in/sec<sup>2</sup> (25.4 mm/sec<sup>2</sup>). The experiments, however, were carried out by applying several displacement amplitudes to the shaker table, and the accelerations induced on the shaker table were measured. The measured values are in general in excess of 1 in/sec<sup>2</sup>, therefore, the test results are scaled down to this value in order to obtain a standard measure for comparison. The maximum and minimum displacements recorded during the sloshing tests are adjusted by the appropriate factor to be compared to those of the computer simulations.

## CONCLUSIONS

The effect of viscosity on the dynamic response of partially-filled liquid storage tanks is studied. Two tank sizes, one small and one large, are modeled using the finite element method. The pressure-velocity formulation built-in the FLUSTR-ANL computer code is employed in simulations. The small tank test cases involve two levels (39% and 78% of the tank height) of liquid (silicone oil) with different viscosity values (1 cP, 200 cP,

and 1000 cP). Similarly, the large tank is filled at 27% and 71% of the tank height, and the liquid viscosities are chosen to be 1 cP, 200 cP, and 1000 cP. Both a seismic excitation (53.76 second El-Centro input with an amplitude of 200 Gal), and harmonic excitations (input frequency equalling the fundamental frequency of each system, and an amplitude of 1 in/s<sup>2</sup> (25.4 mm/s<sup>2</sup>)) are used as input acceleration records. The first and second sloshing frequencies in each case are determined from the simulations under seismic excitation, and the sinusoidal data are created accordingly. The results are presented in terms of tables and time-history/FFT plots for selected nodes and elements in the finite element mesh.

The viscosity is found to manifest itself as a damping effect. The amplitude of surface displacements, and magnitude of dynamic pressures are reduced by an increase in viscosity. However, the sloshing wave form, and the pressure distribution in the liquid are not changed. The most significant reductions are observed in the large tank subjected to resonant harmonic motion. The amplitude of displacements and pressures for the 200 cP case are approximately four times of those for the 1000 cP case. In the small tank cases, the amplification amounts to approximately twice. However, more moderate differences, 25% and 12%, are found for the large and small tanks under seismic excitation, respectively. The broad frequency spectrum characteristics of earthquake records may be the main reason. The fundamental sloshing frequency for each simulation case is virtually unaffected by an increase in viscosity. The slight beating phenomenon observed in the small tank cases makes the identification of the fundamental sloshing frequency more difficult, leading to a variation of approximately 5% between the 1 cP and 1000 cP cases. The sloshing frequencies of the large tank where virtually no beating phenomenon is encountered are even less sensitive (4% for 27% full tank), or totally unaffected (71% full tank).

The computer simulations with input harmonic frequencies near the second sloshing frequency of the fluid-tank cases considered in this study show the same damping characteristics outlined above.

## ACKNOWLEDGMENTS

This work was performed in the Engineering Mechanics Program of the Reactor Engineering Division of Argonne National Laboratory under the auspices of the U.S. Department of Energy under contract W-31-109-Eng-38. The work is related to the design and analysis of HLW storage tanks and was supported by the Office of Hanford Programs (EM-36).

## REFERENCES

- Chang, Y. W., Ma, D. C., and Gvildys, J., 1987, "EPRI/CRIEPI/Joint Program on Seismic Sloshing of LMR Reactors. Part II - Numerical Simulations," *Transactions, SMIRT-9 Conference*, Lausanne, Switzerland, Vol.E, pp. 253-258.
- Chang, Y. W., Ma, D. C., Gvildys, J., and Liu, W. K., 1988, "Seismic Analysis of LMR Reactor Tanks," *Nuclear Engineering and Design*, Vol. 106, pp. 19-33.

Chiba, T., Nakajima, S., Mieda, T., Ogawa, N., and Shibata, H., 1995, "The Sloshing Behavior of High Viscous Liquids in Cylindrical Tanks," *Proceedings, ASME 1995 Pressure Vessel and Piping Conference*, Honolulu, HI, this volume.

Tang, Y., Uras, R. A., and Chang, Y. W., 1993, "Effect of Viscosity on Dynamic Response of a Liquid Storage Tank," *Proceedings, ASME 1993 Pressure Vessel and Piping Conference*, Denver, CO, PVP-Vol. 258, pp. 135-142.

Tang, Y., 1993, "Sloshing Displacements in a Tank Containing Two Liquids," *Proceedings, ASME 1993 Pressure Vessel and Piping Conference*, Denver, CO, PVP-Vol. 258, pp. 135-142.

Table 4. Sloshing Frequencies for Each Configuration of the Large Tank

Liquid Height	Sloshing Frequencies	Viscosity		
		1 cP	200 cP	1000 cP
27%	1st	0.52 Hz	0.51 Hz	0.51 Hz
	2nd	1.05 Hz	1.01 Hz	1.01 Hz
71%	1st	0.61 Hz	0.61 Hz	0.61 Hz
	2nd	1.05 Hz	0.97 Hz	0.99 Hz

Table 1. Tank Specifications and Experimental Setup

	Small Tank	Large Tank
Material	Acrylic	Steel
Inner Diameter (mm)	780	2400
Length (mm)	600	2000
Wall Thickness (mm)	10	6
Liquid Height (%) of Length	78%; 39%	72%; 27%
Number of Level Gauges	3	7
Number of Pressure Gauges	48	56
Number of Acceleration Meters	4	4
Number of Strain Gauges	-	6

Table 2. Specific Density Values of Water and Silicone Oil for Different Viscosities

Specific Density	Viscosity (1 Poise = 1 gr/cm.s; 1 Poise = 100 cP)
1.000	1 cP
0.970	200 cP
0.971	1000 cP

Table 3. Sloshing Frequencies for Each Configuration of the Small Tank

Liquid Height	Sloshing Frequencies	Viscosity		
		1 cP	200 cP	1000 cP
39%	1st	0.97 Hz	0.95 Hz	0.93 Hz
	2nd	1.73 Hz	1.72 Hz	1.73 Hz
78%	1st	1.06 Hz	1.06 Hz	1.04 Hz
	2nd	1.73 Hz	1.72 Hz	1.73 Hz

**DISCLAIMER**

This report was prepared as an account of work sponsored by an agency of the United States Government. Neither the United States Government nor any agency thereof, nor any of their employees, makes any warranty, express or implied, or assumes any legal liability or responsibility for the accuracy, completeness, or usefulness of any information, apparatus, product, or process disclosed, or represents that its use would not infringe privately owned rights. Reference herein to any specific commercial product, process, or service by trade name, trademark, manufacturer, or otherwise does not necessarily constitute or imply its endorsement, recommendation, or favoring by the United States Government or any agency thereof. The views and opinions of authors expressed herein do not necessarily state or reflect those of the United States Government or any agency thereof.

Table 5. Comparison of Selected Simulation and Experimental Results for the Cases Considered in This Study

			Small Tank						Large Tank <sup>1</sup>					
			39%			78%			27%			71%		
			1 cP	200 cP	1000 cP	1 cP	200 cP	1000 cP	1 cP	200 cP	1000 cP	1 cP	200 cP	1000 cP
1st Sloshing Frequency	Frequency (Hz)	FLUSTR	0.97	0.95	0.93	1.06	1.06	1.04	0.52	0.51	0.51	0.61	0.61	0.61
		EXP. <sup>2</sup>	0.98	0.97	-	1.1	1.08	1.06	0.55	0.54	-	0.63	0.62	0.62
	Damping Ratio (%)	FLUSTR <sup>3</sup>	-	1.99	3.97	-	1.46	3.79	-	1.15	3.53	-	0.42	0.6
		EXP.	0.49	1.61	-	0.23	1.17	7.73	0.42	0.64	-	0.13	0.62	1.7
	Maximum Wave Height Under Harmonic Excitation (in.)	FLUSTR	-	0.83	0.42	-	1.14	0.44	-	4.41	1.45	-	12.2	3.02
		EXP. <sup>2</sup>	0.847	0.424	-	0.530	0.43	0.15	1.73	1.35	-	1.46	1.5	0.63
2nd Sloshing Frequency	Frequency (Hz)	FLUSTR	1.73	1.72	1.73	1.73	1.72	1.73	1.05	1.01	1.00	-	0.97	0.99
		EXP.	1.85	1.83	-	1.86	1.84	1.81	1.06	1.05	-	1.06	1.06	1.06
	Maximum Wave Height Under Harmonic Excitation (in.)	FLUSTR	-	0.25	0.045	-	0.098	0.012	-	1.08	0.31	-	1.31	0.38
		EXP. <sup>2</sup>	1.000	0.052	-	0.090	0.129	0.011	0.243	0.125	-	0.404	0.26	0.17
Maximum Wave Height Under Seismic Excitation (in.)	FLUSTR	7.5	6.0	4.2	9.4	5.8	5.1	8.5	7.2	5.6	9.1	8.6	7.0	
	EXP. <sup>2</sup>	5.6	4.2	-	5.4	5.7	2.4	9.6	6.1	-	10.4	8.2	5.0	

<sup>1</sup>Experiments were performed using a large tank filled with 30% and 72% liquid, and computer simulations consider a 27% and a 71% full large tank.

<sup>2</sup>39% full small tank and 27% full large tank with a liquid of 1000 cP were not tested during the experiments.

<sup>3</sup>1 cP harmonic input is not simulated due to the extremely long time it takes to reach its steady state.

**Table 6. Comparison of Time Needed to Reach Steady State in Simulations, and the Duration of Experiments (small tank) (in seconds)**

	Simulations		Experiments	
	1st Mode	2nd Mode	1st Mode	2nd Mode
39%, 200 cP	26	35	30	17
78%, 200 cP	45	40	30	17
39%, 1000 cP	30	15	-	-
78%, 1000 cP	24	15	30	17

**Table 7. Comparison of Time Needed to Reach Steady State in Simulations, and the Duration of Experiments (large tank) (in seconds)**

	Simulations		Experiments		
	1st Mode	2nd Mode		1st Mode	2nd Mode
27%, 200 cP	80	180	30%, 200 cP	58	30
71%, 200 cP	180	180	72%, 200 cP	50	30
27%, 1000 cP	25	35	30%, 1000 cP	-	-
71%, 1000 cP	40	40	72%, 1000 cP	50	30

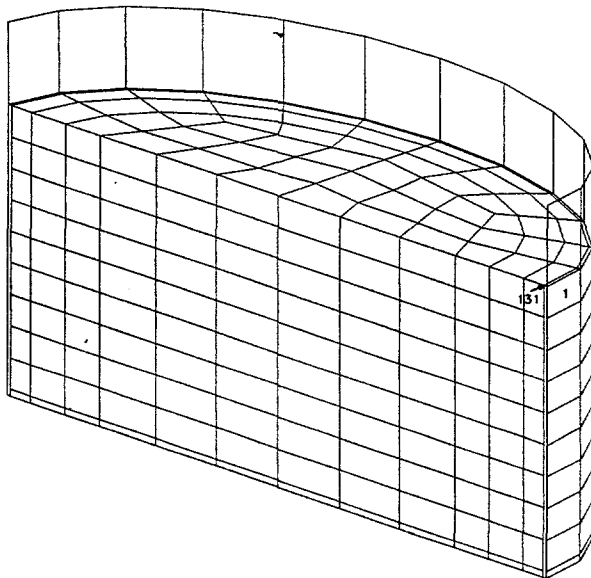
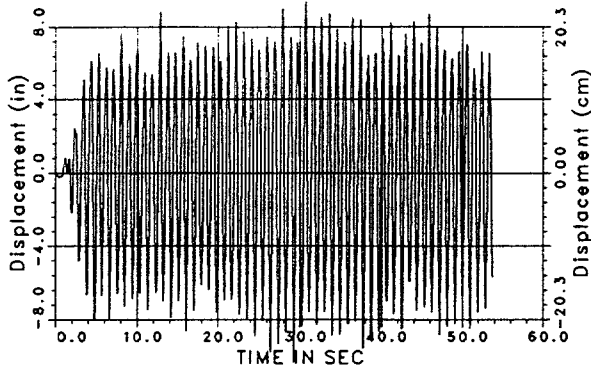


**FIG. 1. FINITE ELEMENT MESH AND NODE/ELEMENT DESIGNATION**

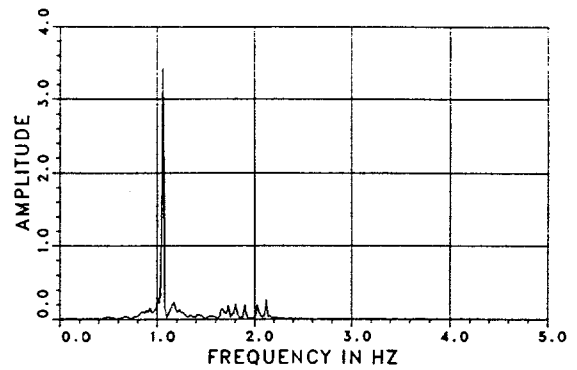
Wave Height at Node 131(Small tank, 78% full, 1cP)

TMAX,AMAX TMIN,AMIN= 30.69 9.4012 29.27 -10.3600



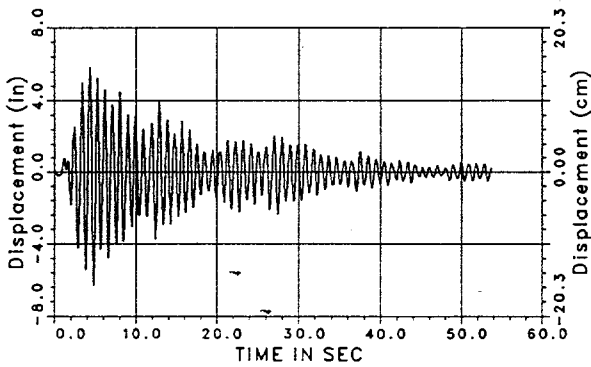
Wave Height at Node 131(Small tank, 78% full)

MAX. FREQUENCY,AMPLITUDE= 1.06 3.4326



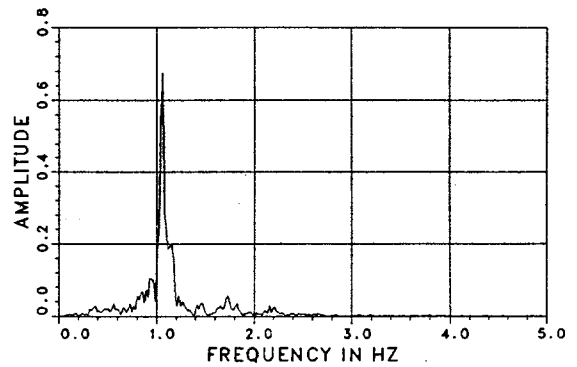
Wave Height at Node 131(Small tank, 78% full, 200cP)

TMAX,AMAX TMIN,AMIN= 4.33 5.8288 4.78 -6.3158



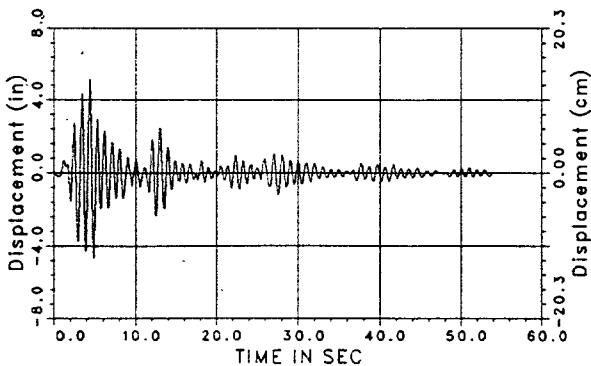
Wave Height at Node 131(Small tank, 78% full)

MAX. FREQUENCY,AMPLITUDE= 1.06 0.6763



Wave Height at Node 131(Small tank, 78% full, 1000cP)

TMAX,AMAX TMIN,AMIN= 4.37 5.1375 4.83 -4.7023



Wave Height at Node 131(Small tank, 78% full)

MAX. FREQUENCY,AMPLITUDE= 1.04 0.2617

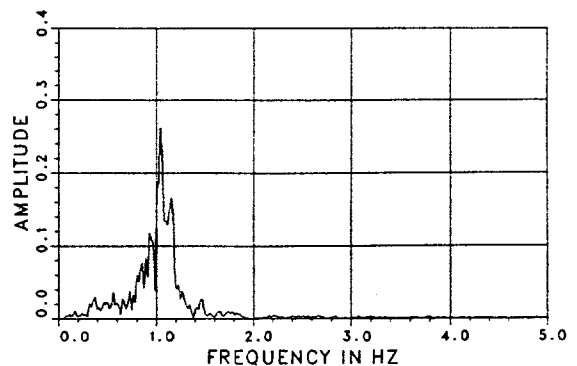
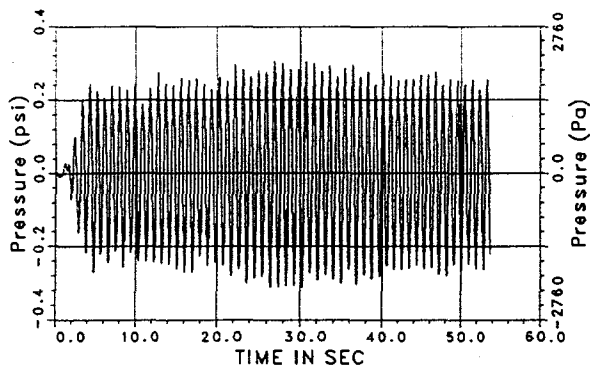
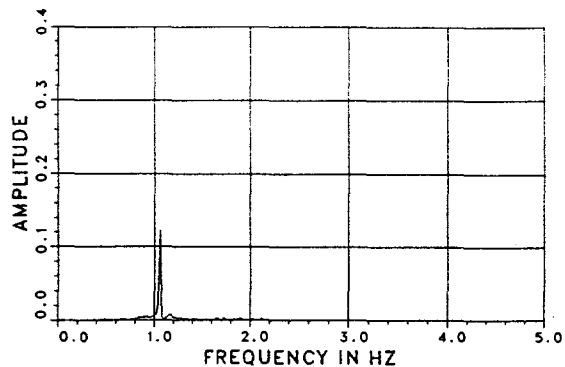


FIG. 2. WAVE HEIGHT VALUES AT NODE 131 OF THE 78% FULL SMALL TANK FOR VISCOSITIES 1 cP, 200 cP and 1000 cP

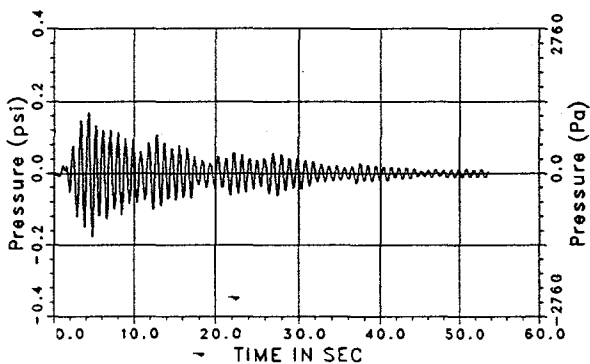
Pressure in Element 1(Small tank, 78% full, 1cP)  
 TMAX,AMAX TMIN,AMIN= 26.90 0.3062 26.43 -0.3116



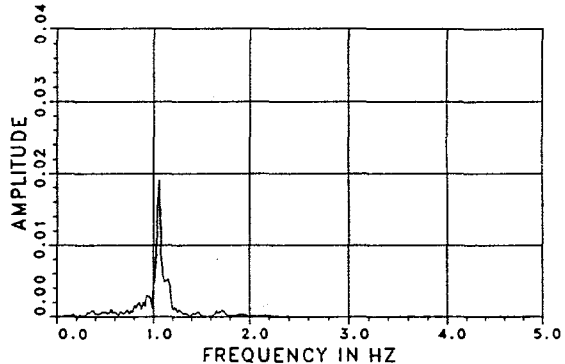
Pressure in Element 1(Small tank, 78% full)  
 MAX. FREQUENCY,AMPLITUDE= 1.06 0.1229



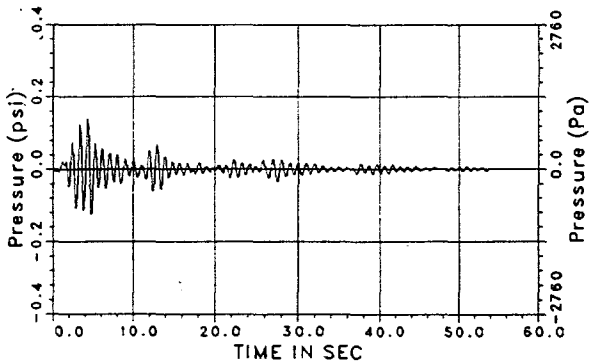
Pressure in Element 1(Small tank, 78% full, 200cP)  
 TMAX,AMAX TMIN,AMIN= 4.30 0.1717 4.75 -0.1763



Pressure in Element 1(Small tank, 78% full)  
 MAX. FREQUENCY,AMPLITUDE= 1.06 0.0190



Pressure in Element 1(Small tank, 78% full, 1000cP)  
 TMAX,AMAX TMIN,AMIN= 4.32 0.1409 4.77 -0.1252



Pressure in Element 1(Small tank, 78% full)  
 MAX. FREQUENCY,AMPLITUDE= 1.04 0.0070

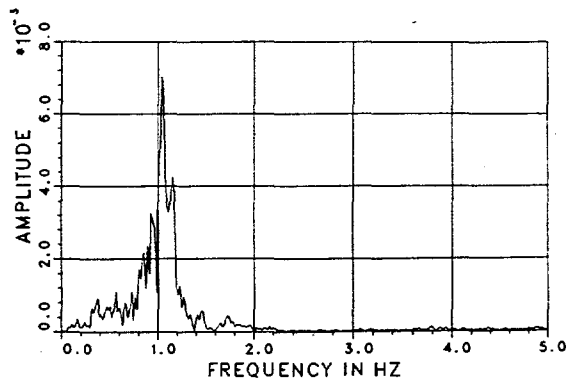


FIG. 3. PRESSURE IN ELEMENT 1 OF THE 78% FULL SMALL TANK FOR VISCOSITIES 1 cP, 200 cP and 1000 cP